Optimal Thermal Unit Commitment Scheme by Including Renewable Energy Sources and Pumped Hydro Energy Storage: Case Study of Niamey Power System, Niger

Issoufou Tahirou Halidou[1*], Mohamed Elsayed Lotfy[1,2], Atsushi Yona[1], Tomonobu Senjyu[1] and Abdoul Aziz Ibrahim[3]

[1]Electrical and Electronics Engineering Department, University of the Ryukyus, Okinawa, Japan
[2]Electrical Power and Machines Department, Zagzig Universty, Egypt
[3]Department of Niamey Power Distribution, Nigerien Society of Electricity, Niamey, Niger
Email: thissoufou@gmail.com

Abstract This paper presents a novel real multi-objective approach for thermal unit commitment (UC) problem solution in Niamey (Niger). The proposed methodology consists of four conventional thermal generating units and imported power from a neighboring country in addition to future inclusion of Photovoltaic (PV) power, Wind Turbine Generators (WTGs), and Pumped Hydro Energy Storage (PHES). Minimization of total daily operating cost and decreasing the maximum daily mismatch between load demand and generation are considered as two objective functions in two cases. In the first case, UC with thermal units considering the imported power (IMP), PV and PHES is determined. In the second case, WTGs are introduced and the IMP is removed in order to get rid of its economical and political problems. ε-MOGA (epsilon Multi-Objective Genetic Algorithm) is used to obtain an optimal unit commitment problem solution with consideration of PV, WTGs and PHES. The effectiveness and robustness of the proposed scheme is verified by numerical simulations using MATLAB environment.

Keywords: Unit Commitment (UC), Photovoltaic Power (PV), Wind Turbine Generators (WTG), Pumped Hydro Energy Storage (PHES), ε-MOGA.

1 Introduction

Niger is a landlocked country in West Africa and a member of the Economic Community of West African States (ECOWAS), as depited in Fig. 1, Niger has a surface area of 1,267,000 square kilometres (km^2), bordering Mali, Burkina Faso and Benin to the West, Nigeria to the South, Chad to the East and Algeria and Libya to the North [1]. Electrically, Niger is highly dependent on imports, covering more than 75% of its national electricity needs. Its power supply is ensured by 5 interconnection lines from Nigeria [2].

Energy is vital for all living-beings on earth. Its availability is one of the basic conditions for the sustainable development and social well being of any nation. However the most usable form of energy is the electrical energy generated by thermal generating units. Generally, the fuel cost for thermal units, transportation cost, storage cost, and so on, are expensive. Therefore, power producers should use an optimal operation of thermal units for operational cost reduction, carbon emission reduction, and for high efficiency. So, Unit Commitment (UC) becomes an important issue. UC is an optimization problem used to determine the operation schedule of the generating units at every hour interval with varying loads under different constraints and environments [3]. [4] conducts a state-of-the-art review on recent literature that have investigated the impacts associated with UC models when high Renewable Energy Sources (RESs) are integrated to the power systems.

In addition, from the population growth in the world which brings the power demand high, the perspective of global warming eradication and depletion of fossil fuels, the application of renewable energies such as photvoltaic (PV) generation and wind generation (WG) in the grid is becoming more widespread, recently. To integrate dispatchable renewables, a two-stage robust UC and dispatch model is established in [5]. In the first stage, a base UC and dispatch is determined. In the second stage, all flexibility resources, such as thermal units and storages including RESs are used to accommodate the uncertainties, which is a Mixed-Integer Programming (MIP) problem. Multi-objective UC approach with

Figure 1. Niger map [1].

renewable energy using hybrid scheme is proposed in [6]. A weighted sum method is applied to convert multi-objective problem to a single one by linear combination of different objectives as a weighted sum and an efficient hybrid algorithm is presented for aiding UC decisions in such environments to minimize the trade-off between the cost and emission objectives. The proposed hybrid approach is a combination of weighted improved Crazy Particle Swarm Optimization (CPSO) with Pseudo code algorithm. Wind scenarios generated by Monte Carlo simulation is utilized to forecast the wind power uncertainty. Fuzzy cardinal approach is used to achieve the best solution of CPSO. The effectiveness of the proposed method is tested on a 10-generator system.

RESs penetration into a given network can provide various benefits to the power companies. To achieve this point, it is required to solve the optimal capacity of the RESs. The technical and economic feasibility of a hybrid energy system integrated with an offgrid power system is investigated in [7]. The methodology involves the use of Hybrid Optimization Model for Electric Renewable (HOMER) for the optimization of the proposed hybrid system. The simulation software package DIgSILENT is used to model and simulate the integration of the proposed hybrid system to the existing network. Different scenarios are considered in both the hybrid system optimization and the assessment of the impact of the hybrid energy system integration implemented different connection scenarios.

However, it is difficult to predict the output power generated by RESs. Their inclusion into the power systems brought major challenges as a result of their output variations. As countermeasures, Pumped Hydro Energy Storage (PHES) is introduced into the power system under study. PHES is a form of energy storage that can quickly respond to mismatches between demand and generation, it can play an important role in mitigating the uncertainty of RES, specially wind power. [8] proposes a robust wind-hydro-thermal UC model that provides reliable day-ahead UC decisions. A deterministic and an interval UC formulation for the co-optimization of controllable generation and PHES, including a representation of the hydraulic constraints of the PHES is proposed in [9]. PHES unit not only has the functions of peak-load regulation and frequency modulation, but also has the capability of fast response and excellent load tracking, which can effectively reduce the installed capacity of thermal power, decrease peak-load regulation depth, improve operational efficiency of the power system [10]. [11] proposes a novel annual analysis for the thermal power generator and pumped storages under a massive introduction of RESs. A weekly UC schedule (start/stop planning) for thermal power generator and pumped storages has been modeled and calculated for one year evaluation. A variety of power generators included in the modeling of this proposed method are thermal power plants (oil, coal, LNG, combined cycle (CC)), hydroelectric power plants

(pump storages, dams, inflow), nuclear power plants, and RES generators (geothermal plants, PVs). To solve the generator start/stop planning problem, Tabu search and interior point methods are adopted to solve the operation planning for thermal power generators and the output decision for pumped storages, respectively. In addition, by assuming load frequency control (LFC) constraints to cope with PV output fluctuations, the impact of the intensity of LFC constraints on the operational cost of the thermal power generator has been elucidated. The increment of the operational cost of the power supply with increasing PV introduction amount has been shown in concrete terms.

Moreover, Energy storage Systems (ESSs) are necessary for power quality improvement in power grids even with the integration of RESs. [12] presents an analysis of a grid scale ESSs integrated with a wind power plant (WPP). Firstly the impact of a distributed generation unit (a wind power plant) to a power grid is analysed and then ESSs of different capacities are integrated to the power grid in an effort to study the improvements in the power quality.

In this paper, an optimization approach for Niamey (Niger) power system comprises of thermal generating units and an IMP with future peneration of PV, WTGS, and PHES is proposed in order to determine an optimal thermal UC problem solution. The objectives of minimizing the total daily operating cost (TDOC) and the reduction of the maximum daily load/generation deficit can be seen from the simulation results. The proposed method uses ε-MOGA for optimization method. The effectiveness of the proposed method is confirmed by simulation results on MATLAB®.

2 Examined Power System Description

The Niamey power system is configured in two cases as follows:

Case 1: The configuration of the proposed model is depicted in Fig. 2. The system consists of the grid (imported power from Nigeria and four conventional thermal generating units), future inclusion of PV array system and PHES, and Niamey power demand.

Case 2: The model is shown in Fig. 3. The model components are the grid (only the four conventional thermal generating units), future penetration of PV array system, WTGs and PHES to meet the changing load, and Niamey load demand.

The generation capacities of imported power and the four diesel generators are 60MW, 19MW, 19MW, 9MW and 2MW, respectively.

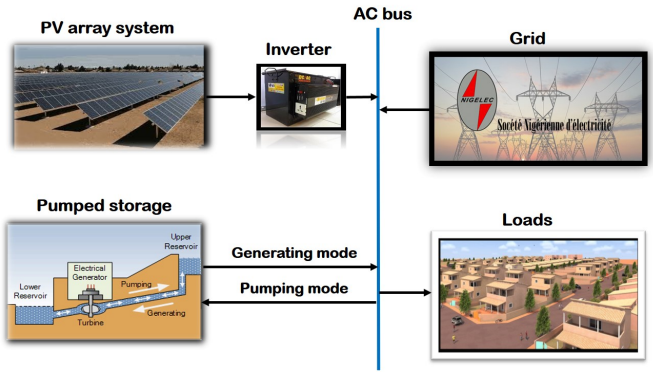

Figure 2. Power system configuration under case 1.

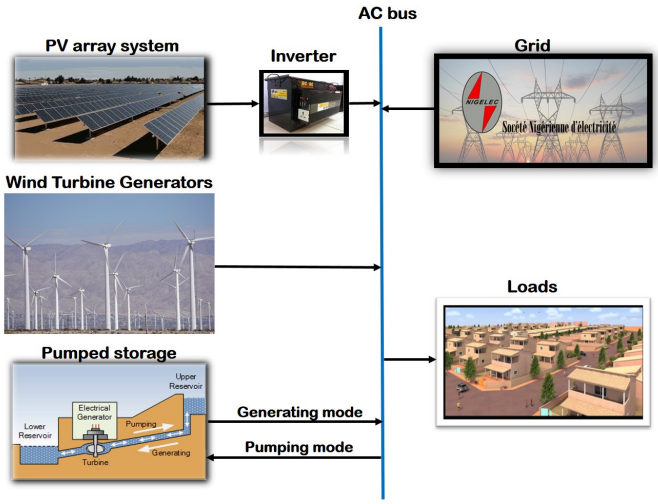

Figure 3. Power system configuration under case 2.

3 Mathematical Modeling

Minimizing the total daily operating cost and decreasing the load-generation deficit are the two objectives considered in this paper. Techno-economic modeling of each component of the system is required in order to achieve the two objectives.

3.1 PV Array System Output Power

The power supplied by a set of PV panels at hour t is as follows [13]:

$$P_{PV}(t) = \eta_{PV}.A_{PV}.S(t). \tag{1}$$

where, η_{PV} represents PV panels efficiency, A_{PV} (m^2) the total area occupied by PV panels, and $S(t)$ (kW/m^2) the hourly solar radiation.

3.2 Wind Turbine Generator Output power

As wind speed increases above cut-in speed (V_{ci}), the power generated by the turbines increases as the cube of wind speed, until reaching a maximum point at rated speed (V_r). This is the rated power (P_{WTG}) in kW for which the wind turbine is designed for. At some point, the wind speed becomes very high, and can cause the wind turbines to be damaged. This is called cut-off speed (V_{co}) [13]. Equation (2) describes the wind turbine generator rated output power at any time t:

$$P_{WTG}(t) = 0.5.C_p.\rho_a.A_W.V_r^3(t). \tag{2}$$

where, C_p is the power coefficient and it is the ratio of the power output of a wind generator divided by maximum power, ρ_a (kg/m^3) is the air density, $V_r^3(t)$ (m/s) the rated wind speed at t^{th} hour, and A_W (m^2) is the total swept area of wind tubine generator blades.

3.3 Pumped Hydro Energy Storage (PHES)

The PHES subsystem consists of a turbine/generator unit and a pump/motor unit. The volume of the Upper Reservoir (UR) and the height difference between the upper and lower reservoir are the most important two variables which are observed in literature [14]. In this paper, the height difference is fixed at 60m, and the Niger river is considered as the lower reservoir.

Generating mode: turbine/generator unit : During energy deficit periods, the output from the turbine/generator unit is [15], [16]:

$$P_t(t) = \eta_t \ . \ \rho \ . \ g \ . \ h \ . \ q_t(t) = c_t \ . q_t(t). \tag{3}$$

where η_t is the overall efficiency of the turbine/generator unit ρ is the water density (=1000kg/m^3); g is the gravitational acceleration (=9.81 m/s^2), h is the elevating height (m), $q_t(t)$ is the water volumetric flow rate input into the turbine (m^3/s) at time t and c_t the turbine generating coefficient (kWh/m^3).

Pumping mode: pump/motor unit : The water flow rate elevated from the lower reservoir by the pumps is expressed in Equation (4). The power source in the pumps is directly supplied by the hybrid grid and renewable energy sources. The water pumping can be compared to the charging rate of battery bank [15], [16].

$$q_p(t) = \frac{\eta_p \ . \ P_p(t)}{\rho \ . \ g \ . \ h} = c_p \ . \ P_p(t). \tag{4}$$

where η_p is the overall pumping efficiency; $P_p(t)$ is the input power from the hybrid grid and RESs power generators to the pump at time t; and c_p is the water pumping coefficient of the unit (m^3/kWh).

Upper Reservoir (UR) : The water quantity stored in the UR should be enough to meet the power demand of the system during peak load demand and insufficient hybrid energy generators. The quantity of water stored in the UR at any time t is determined by [15], [16]:

$$V_{UR}(t) = V_{UR}(t-1)(1-\alpha) + q_p(t) - q_t(t). \tag{5}$$

where α is the evaporation and leakage loss. α is similar to the self-discharge of battery bank and it is neglected for simplifying the calculations. The water level in the UR can be considered as the state of charge (SOC) of the storage tank.

$$SOC(t) = \frac{V_{UR}(t)}{V_{UR_{max}}}. \tag{6}$$

where $V_{UR_{max}}$ is the maximum water quantity stored in the UR.

3.4 Power Generation Modeling

The amount of power generated by the grid, renewable energy sources and pumped storage generators at hour t is as follows:

$$P_G(t) = P_{Grid}(t) + P_{RES}(t) - P_p(t). \tag{7}$$

$$P_G(t) = P_{Grid}(t) + P_{RES}(t) + P_t(t). \tag{8}$$

where $P_{Grid}(t)$, $P_{RES}(t)$, $P_p(t)$, and $P_t(t)$ are the power output from the grid, the renewable energy sources, power delivered to the pump-motor unit during charging mode, and power from the turbine-generator unit during discharging mode at time t respectively.

Two cases are considered in this study:

Case 1 :

PV is only considered here as the renewable energy sources as shown in Equation (9). Also, the grid composes of the four conventional thermal generating units and the imported power as shown in Equation (10).

$$P_{RES}(t) = P_{PV}(t). \tag{9}$$

$$P_{Grid}(t) = P_{DG}(t) + P_{IMP}(t). \tag{10}$$

where, $P_{PV}(t)$, $P_{DG}(t)$, and $P_{IMP}(t)$ are the power output from the PV array system, the four diesel generators and the imported power at time t respectively.

Case 2 :

Equation (11) describes that the renewable energy sources considered are PV and WTGs. In this case, the grid composes only of the four conventional thermal generating units as shown in Equation (12). Here the imported power is being discarded.

$$P_{RES}(t) = P_{PV}(t) + P_{WTGs}(t). \tag{11}$$

$$P_{Grid}(t) = P_{DG}(t). \tag{12}$$

where, $P_{WTGs}(t)$ is the power output from the wind turbine generator at t hour.

4 Formulation

In this section, objective functions are formulated, economic analyse are made, constraints are expressed, and optimization technique is described.

4.1 Objective Functions

The two states of pumped storage are simulated with virtual generator and virtual motor [17]. Taken the total daily operating cost of conventional thermal generating units, imported power, and renewable energy sources, and maximum daily load-generation deficit minimum as objects, by considering the states switching costs of pumped storage, the objective functions are defined in two cases as follows:

For case1:
Total daily operating cost

$$min : TDOC = Cost(P_{DG} + P_{IMP} + P_{PV} + P_p). \tag{13}$$

Load-generation deficit

$$min : [max(generation - load)]. \tag{14}$$

For case2:
Total daily operating cost

$$min : TDOC = Cost(P_{DG} + P_{PV} + P_{WTGs} + P_p). \tag{15}$$

Load-generation deficit

$$min : [max(generation - load)]. \tag{16}$$

4.2 Economic Analyses

The life cycle cost (LCC) of RESs and PHES are obtained as follows:

PV array LCC : The capital cost of the investment for PV array system is equal to the initial cost (α_{PV} in \$/m^2) of PV array multiplied by the total area (A_{PV} in m^2) occupied by PV array [13-18]:

$$C_{PV} = \alpha_{PV}.A_{PV}. \tag{17}$$

The total operation and maintenance cost of PV array per year is:

$$OM_{npv,PV} = \beta_{PV}.A_{PV}.\sum_{j=1}^{N}\left(\frac{1+\mu_{PV}}{1+i}\right)^j. \tag{18}$$

Table 1. Parameters used

Interest rate	i	0.1
Project lifetime	N (years)	20
Inflation rate	δ	0.04
Escalation rate	$\mu_{pv,w,p}$	0.075
PV initial cost	α_{PV} (\$/m^2)	519.7
Annual O & M cost of PV	β_{PV} (\$/m^2/year)	1% of α_{PV}
Resale price of PV	λ_{PV} (\$/m^2)	25% of α_{PV}
PV efficiency	η_{PV}	16%
Lifetime of PV	L_{PV} (years)	20
Initial cost of wind turbine	α_W (\$/m^2)	544.2
Annual O & M cost of wind turbine	β_W (\$/m^2/year)	2% of α_W
Resale price of wind turbine	λ_W (\$/m^2)	30% of α_W
Wind turbine lifetime	L_W (years)	20
Wind power coefficient	C_p	0.59
Air density	ρ_a (kg/m^3)	1.225
Reinforce concrete (reservoir)	α_{UR} (\$/m^3)	170
Pump initial cost	α_p (\$/kW)	238.866
Pump lifetime	L_p (years)	10
Turbines and pipes	$\alpha_{t\&pi}$ (\$/kW)	1000
Turbines and pipes lifetime	$L_{t\&pi}$ (years)	10

where, β_{PV} is the annual operation and maintenance cost (\$/m^2/year), μ_{PV} the annual rate, i is the interest rate and N denotes the project lifetime.

By assuming the lifetime span of PV panels equal to the project lifetime, the total replacement cost for PV panels is zero ($R_{PV} = 0$).

By considering the resale price of λ_{PV} (\$/m^2), the total income obtained from resale is [13-18]:

$$S_{npv,PV} = \lambda_{PV}.A_{PV}.\left(\frac{1+\delta}{1+i}\right)^N. \tag{19}$$

where, δ denotes the inflation rate.

Finally, the life cycle cost of PV array is obtained by using Equation (20) [13-18]:

$$LCC_{PV} = C_{PV} + OM_{npv,PV} + R_{npv,PV} - S_{npv,PV}. \tag{20}$$

where, C_{PV}, OM_{PV}, R_{PV}, and S_{PV} are the capital cost, operation and maintenance cost, replacement cost, and salvage cost (in \$) respectively. The subscript *npv* represents the net present value of each factor.

WTGs LCC : The wind turbine generators life cycle cost is obtained using the same equations as for the PV array, except that the subscript PV is replaced by WTGs.

LCC of PHES major component : The cost of upper reservoir (UR) is mainly from the reinforced concrete. Similarly, the LCC value for the UR is obtained using the same equations as for the PV array, except that the subscript PV is replaced by UR.

Table 1 above presents the parameters used in this study.

4.3 Constraints

In minimizing the objective function regarding the total daily operating cost, the following system constraints must be satisfied:

Pumped Storage Constraints a) Generation limit constraints:

$$P_{g\ min,k} \leq P_{g,k,t} \leq P_{g\ max,k}. \tag{21}$$

$$P_{p\ min,k} \leq P_{p,k,t} \leq P_{p\ max,k}. \tag{22}$$

where, $P_{g\ min,k}$ and $P_{g\ max,k}$ are the minimum and maximum output powers from the pump k during the generating mode at time t respectively. $P_{p\ min,k}$ and $P_{p\ max,k}$ are the minimum and maximum output powers consumed by the pump k during the pumping mode at time t respectively.

b) Water flow limit constraints:

$$Q_{g\ min,k} \leq Q_{g,k,t} \leq Q_{g\ max,k}. \tag{23}$$

$$Q_{p\ min,k} \leq Q_{p,k,t} \leq Q_{p\ max,k}. \tag{24}$$

where, $Q_{g\ min,k}$ and $Q_{g\ max,k}$ are the minimum and maximum water flow rates in pump k during the generating mode at time t respectively. $Q_{p\ min,k}$ and $Q_{p\ max,k}$ are the minimum and maximum water flow rates in pump k during the pumping mode at time t respectively.

c) Upper level limit of a reservoir:

$$V_{u\ min,k} \leq V_{u,k,t} \leq V_{u\ max,k}. \tag{25}$$

where, $V_{u\ min,k}$ and $V_{u\ max,k}$ are the minimum and maximum water volume (m^3) in the upper reservoir at time t respectively.

d) Water balance between the upper and lower reservoir:

$$V_{u,k,t+1} = V_{u,k,t} - Q_{k,t}. \tag{26}$$

$$V_{l,k,t+1} = V_{l,k,t} + Q_{k,t}. \tag{27}$$

Thermal power unit constraint

$$P_{i\ min} \leq P_i^t \leq P_{i\ max} \tag{28}$$

where, $P_{i\ min}$ and $P_{i\ max}$ are the minimum real power generated and maximum real power generated by i^{th} thermal unit in t^{th} hour respectively.

4.4 Optimization Technique

ε-MOGA is an elitist multi-objective evolutionary algorithm based on the concept of epsilon-dominance, which is used to control the content of the archive A(t) where the result of the optimization problem is stored [19]. ε-MOGA obtains an ε-pareto set, Θ_p^* (which is not unique), that converges toward the pareto optimal set, Θ_p in a smart distributed manner around the pareto front $\mu(\Theta_p)$ with limited memory resources. Moreover, it adjusts the limits of the pareto front dynamically and prevents the solutions belonging to the ends of the front from being lost. To reach this goal, the objective space is split into a fixed number of boxes n_box_i. So, for each dimension i ϵ [1....n], n_box_i cells of ε_i width are created [20]:

$$\varepsilon_i = (\mu_i^{max} - \mu_i^{min})/n\_box_i, \mu_i^{max} = max\mu_i(x)m,$$
$$\mu_i^{min} = min\mu_i(x) and\ x\ \epsilon\Theta_p^*. \tag{29}$$

This grid preserves the diversity of $\mu(\Theta_p^*)$ since each box can be occupied by only one solution. For a solution x ϵ solution space, $box_i(x)$ can be defined by

$$box_i(x) = ([(\mu_i(x) - \mu_i^{min})/(\mu_i^{max} - \mu_i^{min})] \\ *[n\_box_i]) \ . \tag{30}$$

$\forall\ i\ \epsilon\ [1.....n]$

A solution x^1 with value $\mu(x^1)$ ε-dominates the solution x^2 with value $\mu(x^2)$, denoted by $x^1 <_\varepsilon x^2$, if and only if

$$box(x^1) < box(x^2) \vee (box(x^1) < box(x^2) \wedge x^1 < x^2),$$

$$box(x) = box_1(x), ..., box_s(x). \tag{31}$$

Hence, a set $\Theta_p^* \subseteq \Theta_p$ is ε-pareto, if and only if

$$\forall\, x^1, x^2\, \epsilon\, \Theta_p,\ x^1 \neq x^2, \\ box(x^1) \neq box(x^2) \wedge box(x^1) >_\varepsilon box(x^2). \tag{32}$$

Therefore, ε-MOGA updates A(t) by saving only ε-dominant solutions that do not share the same box. When two mutually ε-dominant solutions compete, the solution that remains in A(t) is the closer to the center of the box. So, preventing solutions belonging to adjacent boxes and increasing diversity of solution can be achieved. The algorithm is composed of three populations: the main population, P(t), which explores the search space D_s during the iterations and its population size is $Nind_p$. The auxiliary population G(t) and its size is $Nind_G$, which must be an even number. The last one is the archive, A(t), which stores the solutions Θ_p^* and its size is $Nind_A$ that is variable but bounded by:

$$Nind\_max\_A = \frac{\prod_{i=1}^{s}(n\_box_i + 1)}{n\_box_{max} + 1}. \tag{33}$$

where n_box_{max}= max[n_box_1,....,n_box_s].
The main steps of the proposed algorithm are as follows [21-24]:

- Step1. Begin and create empty A(t).
- Step2. P(0) is initialized with $Nind_p$ individuals that have been randomly selected from D_s.
- Step3. Calculate the fitness value of each individual in P(t).
- Step4. Check individuals in P(t) that might be included in A(t), as follows:
  - 1) Non-dominated individuals in P(t) are detected, Θ_{ND}.
  - 2) Pareto front limits μ_i^{max} and μ_i^{min} are calculated from μ(x),$\forall$ x ϵ Θ_{ND}.
  - 3) Individuals in Θ_{ND} are analyzed and those which are not ε-dominated by individuals in A(t), are included in A(t).
- Step5. Create G(t) as follows:
  - 1) Two individuals are randomly selected, x^p from P(t), and x^A from A(t).
  - 2) A random number u ϵ [0-1] is generated.
  - 3) If u > $P_{c/m}$ (probability of crossing/mutation), x^p and x^A are crossed over by means of the extended linear recombination technique.
  - 4) If u < $P_{c/m}$, x^A and x^p are mutated using Gaussian distribution and then included in G(t).

  This procedure is repeated $Nind_p/2$ times until G(t) is filled up.
- Step6. Calculate the fitness value of each individual in G(t).
- Step7. Check, one by one, which individuals in G(t) must be included in A(t) on the basis of their location in the objective space.
- Step8. Update P(t) with individuals from G(t). Every individual x^G from G(t) replaces an individual x^p that is randomly selected from the individuals in P(t) which are dominated by x^G. However, x^G will not be included in P(t) if there is no individual in P(t) dominated by x^G.

Finally, individuals from A(t) compose the smart characterization of the pareto front , Θ_p^* .

5 Results and Discussion

5.1 Results

The optimization results using ε-MOGA are presented in this section.

A. Case 1

Fig. 4 provides the Pareto Front. The PV output power and the water volume stored in the upper reservoir are depicted in Fig. 5 and Fig. 6 respectively. Fig. 7 and Fig. 8 present the power taken from the hybrid grid and the output power supplied by the pumps to the combined thermal units, imported power and PV array system, respectively. The load/generation balance is shown in Fig. 9.

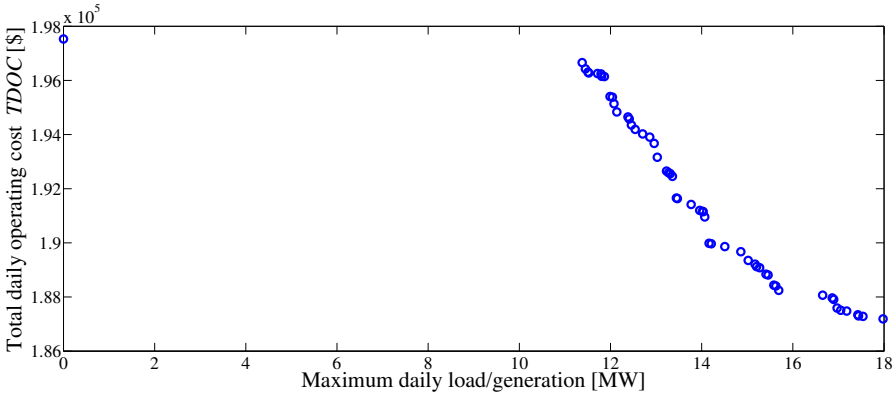

Figure 4. Pareto-Front.

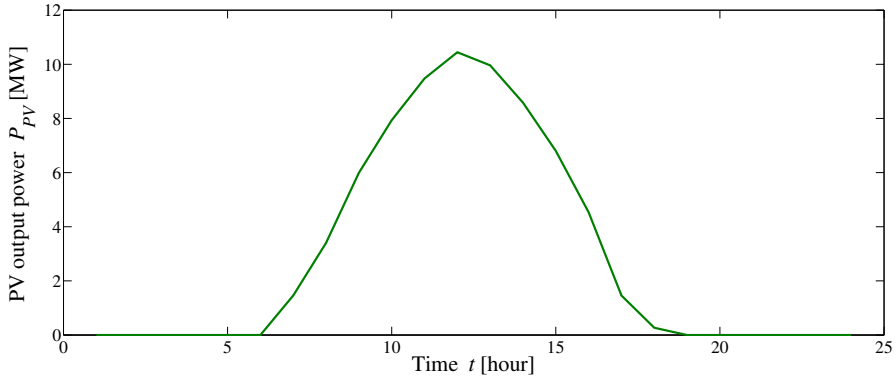

Figure 5. PV output power.

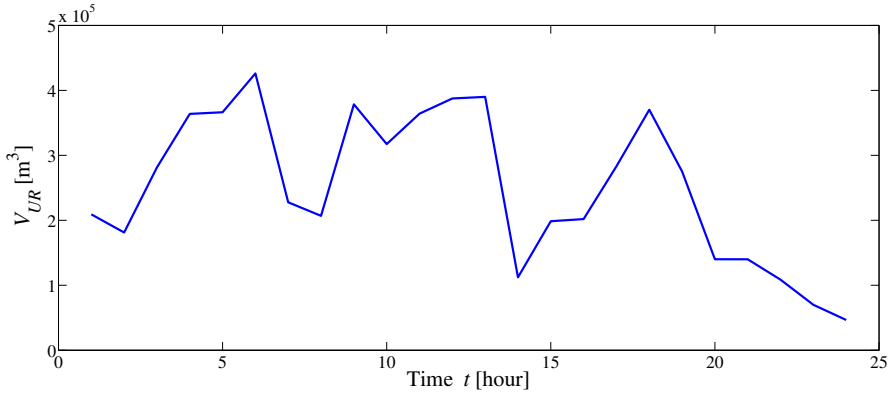

Figure 6. Water volume in the upper reservoir.

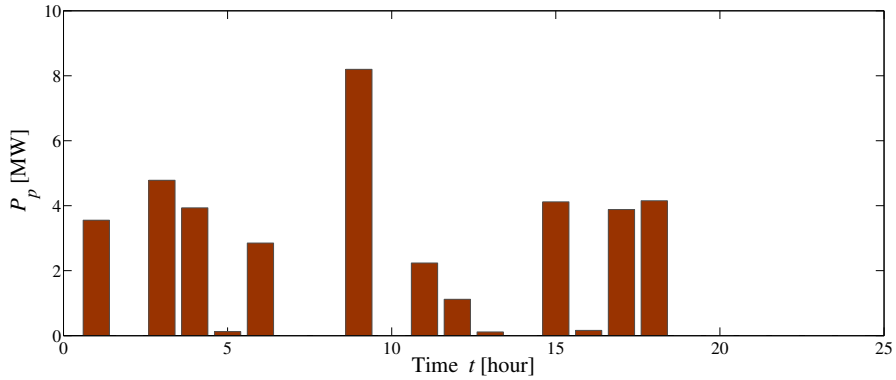

Figure 7. Output power for pumping water.

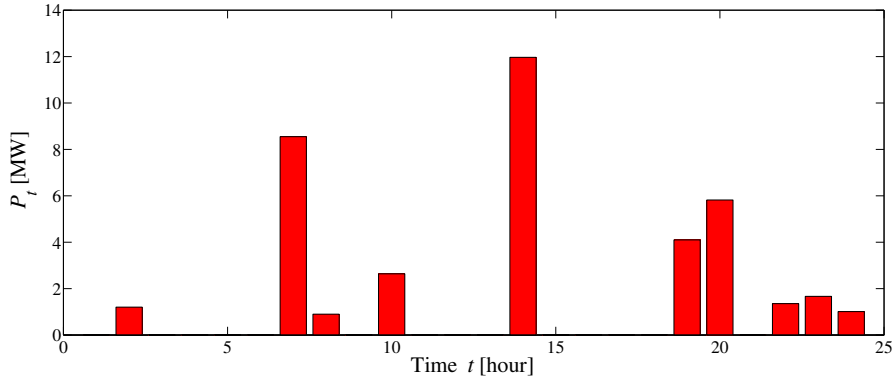

Figure 8. Output power from the pumps.

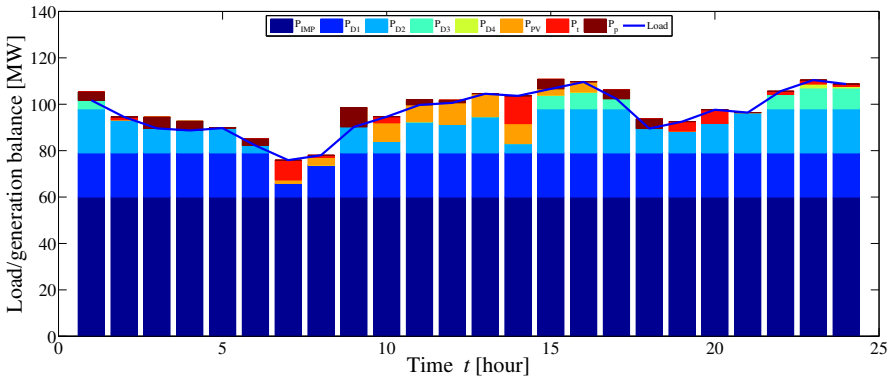

Figure 9. Load generation balance curves.

B. Case 2

The Pareto Front is shown in Fig. 10. Fig. 11, Fig. 12 and Fig. 13 present the PV output power, the wind turbine generators output power, and the volume of water contained in the upper reservoir used in optimization, respectively. The output power for pumping water in case of less load demand is shown in Fig. 14 while Fig. 15 provides the output power supplied by the thermal units, PV array system and WTGs during high load demand. Fig. 16 depicts the load/generation balance.

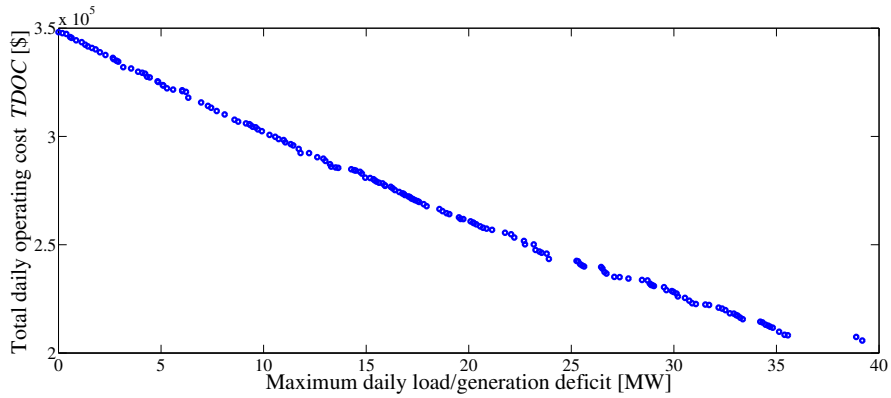

Figure 10. Pareto-Front.

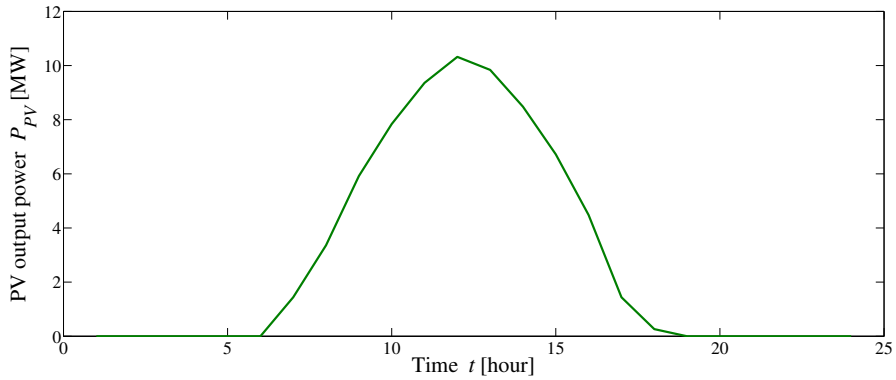

Figure 11. PV output power.

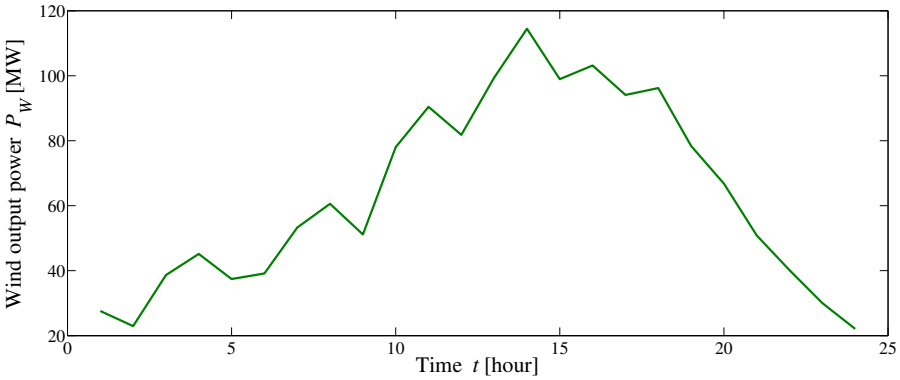

Figure 12. Wind turbine generators output power.

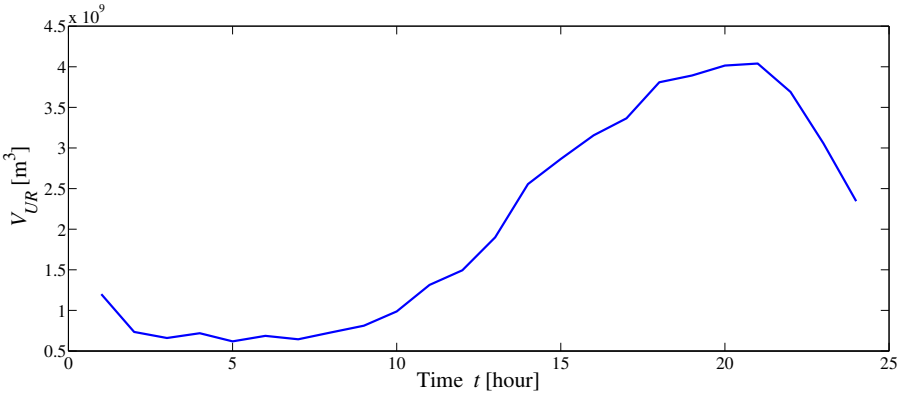

Figure 13. Water volume in the upper reservoir.

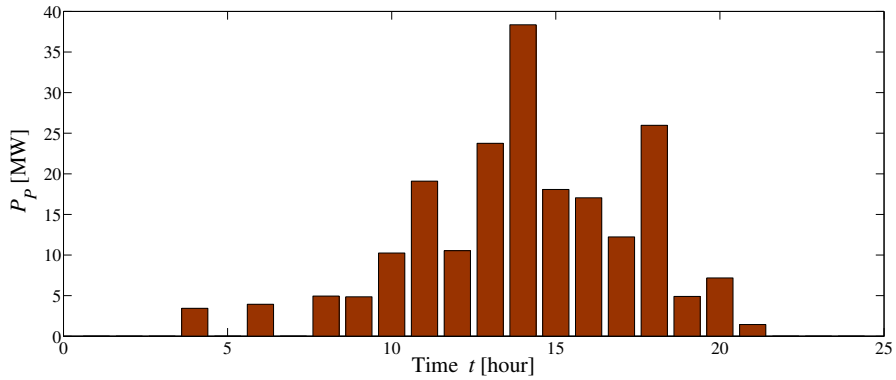

Figure 14. Output power for pumping water.

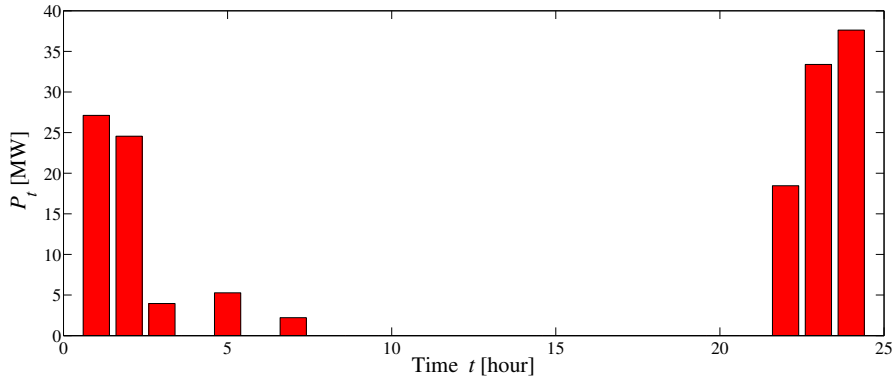

Figure 15. Output power from the pumps.

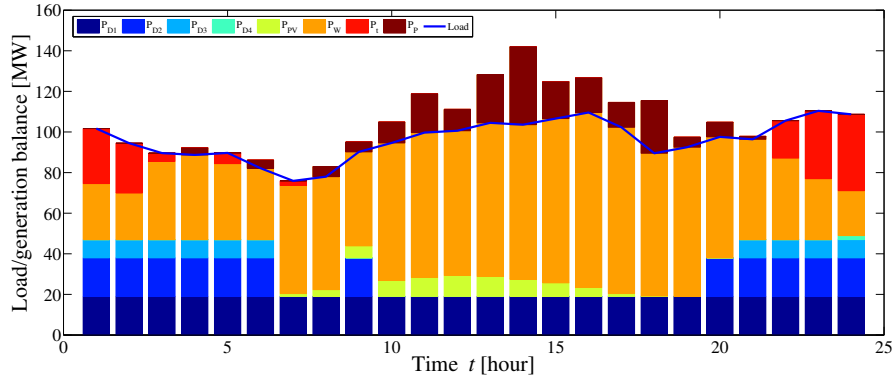

Figure 16. Load generation balance curves.

5.2 Discussion

ε-MOGA is used to optimize the values of decision variables in order to solve the UC problem using renewable energy sources and pumped storage into two cases as follows:

A. Case 1

In this approach, ε-MOGA is applied to tune 98 decision variables consisting of the area of PV panels, water volume in the upper reservoir, and the hourly output power of each diesel generator. The parameters of the algorithm were set to:

$Nind_G = 8$, $Nind_P = 50000$, $P_{c/m} = 0.2$, $Number\ of\ generation = 1000$, $n\_box_1 = n\_box_2 = 500$.

After running the simulation of the proposed optimization scheme, the final Pareto Front of ε-MOGA is achieved which consists of 29 points as shown in Fig. 4. Considering the priority of the first objective to meet the load demand while minimizing the total daily operating cost, one point is selected to achieve the proposed performance. In this study, the quantity of water contained in the upper reservoir (Fig. 6) is set to 5% as minimum storage capacity, and the maximum storage capacity 95%. However, in case of off peak load demand, the pump/motor unit (Fig. 7) takes surplus power from the hybrid grid and PV array system in order to pump water from the river to the upper reservoir. Moreover, power output from the turbine/generator unit (Fig. 8) comes into action during peak load demand. These two figures are referred to as pumping mode and generating mode respectively, which are like the charging/discharging scenario of batteries. Furthermore Fig. 9 indicates the load/generation balance where the total generation (IMP, DGs, PV, and PHES) succeeded to meet the load demand (peak load) when PHES is in generating mode. It is worthy to be mentioned that wherever we observe the brown bar above the load curve for certain hours, it means that the power demand is less than the generated power. This surplus power is being used by the PHES to pump water into the upper reservoir.

B. Case 2

Wind turbine generators are used in this case beside photovoltaic power to replace the imported power. The proposed scheme is expected to be as long run plan to get rid of the economical and political problems of the imported power. ε-MOGA is utilized to optimize 99 decision variables consisting of the area of PV panels, area of wind turbine generators, water volume in the upper reservoir, and the hourly output power of each diesel generator. The same two objective functions of case 1 are considered. The parameters of the algorithm in this case were set to:

$Nind_G = 8$, $Nind_P = 70000$, $P_{c/m} = 0.2$, $Number\ of\ generation = 1000$, $n\_box_1 = n\_box_2 = 500$.

Pareto Front of ε-MOGA is achieved after running the simulation of the proposed optimization technique containing 171 points as shown in Fig. 10. One point is then selected to achieve the proposed behaviour considering the priority of the first objective function. As mentioned in the results section, Fig.14 describes the power supplied by the hybrid thermal units and renewable energy sources to the pumps during off peak load and Fig. 15 represents the amount of power delivered by the pumps during peak load demand. In addition, Fig. 16 presents the load/generation balance where the total generation (DGs, WTGs, PV, and PHES) succeeded to meet the load demand. Finally, this case shows the independence of the Niamey power system from the imported power.

6 Conclusion

This paper presents a modern real multi-objective scheme to solve the thermal unit commitment problem in Niamey, the capital of Niger. Two scenarios are considered in the proposed approach. The first scenario consists of the inclusion of PV and PHES with four conventional thermal generating units and imported power from a neighboring country. Moreover, in the second scenario, WTGs are utilized beside PV and PHES to get rid of the imported power and its economical and political effects. Minimizing the total daily operating cost and reducing the maximum daily load/generation deficit are considered as two objective functions in the two cases and ε-MOGA is used to tune the values of the decision variables in the two scenarios according to the proposed objective functions. The effectiveness and robustness of the proposed control methodology for meeting the load, minimizing the total daily operating cost, and solving the unit commitment problem for the diesel generators over the day with the inclusion of PV, WTGs and PHES is confirmed through the two scenarios using MATLAB® environment.

Acknowledgments. For this paper, the authors would like to thank the University of the Ryukyus through the African Business Education Initiative (ABE Initiative).

References

1. S. Gauri, A.N Safiatou, and M.Y Sokona, "NIGER RENEWABLES READINESS ASSESSMENT", *International Renewable Energy Agency (IRENA)*, pp. 1-2, 2003.
2. S. Gado, "The Energy Sector of Niger: Perspectives and Opportunities", *Energy Charter Secretariat Knowledge Centre*, pp. 9-10, 2015.
3. B. Saravanan, S. Das, S. Sikri, and D.P Kothari, "A solution to the unit commitment problem-a review", *Front.Energy*, vol. 7, no. 2, p. 223, 2013.
4. S.Y. Abujarad, M.W. Mustafa, and J.J. Jamian, "Recent approaches of unit commitment in the presence of intermittent renewable energy resources: A review", *Renewable and Sustainable Energy Reviews*, vol. 70, pp. 215-223, 2017.
5. Y. Hongxing, J. Wang, G. Yinyin, J. Li, and Z. Li, "Robust Integration of High-level Dispatchable Renewables in Power System Operation", *IEEE Transactions on Sustainable Energy*, vol. 8, no. 2, pp. 826-835, 2017.
6. A. Shukla, and S.N. Singh, "Multi-objective Unit Commitment with Renewable Energy using Hybrid Approach", *The Institution of Engineering and Technology (IET Renewable Power Generation)*, vol. 10, no. 3, pp. 327-338, 2016.
7. H.M. Al Ghaithi, G.P. Fotis, and V. Vita, "Techno Economic Assessment of Hybrid Energy Off-Grid System - A Case Study for Masirah Island in Oman", *International Journal of Power and Energy Research*, vol. 1, no. 2, pp. 103-116, July 2017.
8. Y. Chen, F. Liu, W. Wei, S. Mei, and N. Chang, "Robust Unit Commitment for Large-scale Wind Generation and Run-off-river Hydropower", *CSEE Journal of Power and Energy Systems*, vol. 2, no.4, pp. 66-75, 2016.
9. K. Bruninx, Y. Dvorkin, E. Delarue, H. Pandzic, W. D'haeseleer ,and D.S Kirschen, "Coupling Pumped Hydro Energy Storage With Unit Commitment", *IEEE Transactions on Sustainable Energy*, vol. 7, no. 2, pp. 786-796, 2016.
10. N. Shi, S. Zhou, X. Su, R. Yang, and X. Zhu, "Unit Commitment and Multi-Objective Optimal Dispatch Model for Wind-hydro-thermal Power System with Pumped Storage", *2016 IEEE 8th International Power Electronics and Motion Control Conference (IPEMC-ECCE Asia), Hefei, China.*, pp. 1-3, 2016.
11. T. Mitani, M. Aziz, T. Oda, A. Uetsuji, Y. Watanabe, and T. Kashiwagi "Annual Assessment of Large-Scale Introduction of Renewable Energy: Modeling of Unit Commitment Schedule for Thermal Power Generators and Pumped Storages", *Energies*, vol.10, no. 06, pp. 1-19, 2017.
12. A. Neito, V. Vita, and T.I. Maris, "Power Quality Improvement in Power Grids with the Integration of Energy Storage Systems", *International Journal of Engineering Research & Technology (IJERT).*, vol. 5, no. 07, pp. 438-443, July 2017.
13. M.M. Sediqi, M. Furukakoi, M.E Lotfy, A. Yona, and T. Senjyu "Optimal Economical Sizing of Grid-Connected Hybrid Renewable Energy System", *Journal of Energy and Power Engineering*, vol.11, pp. 244-253, 2017.
14. T. Kousksou, P. Bruel, A. Jamil, T. El Rhafiki, and Y. Zeraouli , "Energy Storage: applications and challenges", *Solar Energy Materials and Solar Cells*, vol. 120, Part A, pp. 59-80, 2014.
15. T. Ma, H. Yang, L. Lu, and J.Peng, "Pumped storage-based standalone photovoltaic power generation system: Modeling and techno economic optimization", *Applied Energy*, vol. 137, pp. 649-659, 2015.
16. T. Ma, H. Yang, L. Lu, and J. Peng, "Technical feasibility study on a standalone hybrid solar-wind system with pumped hydro storage for a remote island in Hong Kong", *Renewable Energy*, vol. 69, pp. 7-15 2014.
17. F. Xu, J. Lui, T. Zhang, Q. Ding, and M. Tu, "Unit commitment problem with pumped-storage units[J]", *Automation of Electric Power System*, vol. 36, no. 12, pp. 36-40, 2012.
18. A. Askarzadeh, and L. Dos Santos Coelho, "A novel framework for optimization of a grid independent hybrid renewable energy system: A case study of Iran", *Solar Energy*, vol. 112, pp. 383-396, 2015.
19. J. Herrero, "Non-linear robust identiĭnĄcation using evolutionary algorithms", *Ph.D. Thesis, Polytechnic Univ. Valencia*, 2006.
20. M. Laumanns, L. Thiele, K. Deb, and E. Zitzler, "Combining convergence and diversity in evolutionary multi-objective optimization", *Evolutionary computation*, vol. 10, no. 3, pp. 263-282, 2002.
21. M.E Lofty, T, Senjyu, M.A Farahat, A.F Abdel-Gawad, and A. Yona, "A Frequency Control Approach for Hybrid Power System Using Multi-Objective Optimization", *Energies*, vol. 10, pp. 1-22, 2017.
22. J.M Herrero, G.R Meza G, M. Martinez, X. Blasco, and J. Sanchis, "A Smart-Distributed Pareto Front Using the ev-MOGA Evolutionary Algorithm", *International Artificial Intelligence Tools*, vol. 23, no. 2, pp. 1450002-1-1450002-22, 2014.

23. J.M. Herrero, X. Blasco, M. Martinez, and J. Sanchis, "Multiobjective Tuning of Robust PID Controllers Using Evolutionary Algorithms", *Lecture Notes in Computer Science*, pp. 515-524, 2008.
24. J.M. Herrero, X. Blasco, J. Sanchis, J.V Sanchez-Perez, and J. Redondo, "Design of sound phase diffusers by means of multiobjective optimization approach using ev-MOGA evolutionary algorithm", *Struc. Multidisciplinary Optim.*, vol. 53, no. 4, pp. 861-879, 2016.